

Bis(2-aminobutanol)dichloroplatinum(II) Complexes and Their Singly and Doubly Ring-Closed Butanolato Species – Novel Prodrugs for Platinum-Based Antitumour Chemotherapy?

Markus Galanski,^{*,[a]} Christian Baumgartner,^[a] Vladimir Arion,^[a] and Bernhard K. Keppler^[a]

Keywords: Antitumour agents / Bioinorganic chemistry / N,O ligands / Platinum

Cytotoxic hydroxyethyl-substituted (amine)platinum(II) and -(IV) complexes have recently attracted attention because of the ability of their hydroxyethyl groups to coordinate through the oxygen atom to the platinum centre during oxidation with hydrogen peroxide or through intramolecular ligand exchange reactions in dichloroplatinum(II) complexes. The last point in particular is of great interest, because the intramolecular attack of the hydroxy group dramatically influences the mode of action of platinum(II) compounds. On the other hand, there is also the chance to use such reactions specifically for the synthesis of novel anticancer platinum-based drugs for chemotherapy. We have therefore focused our chemistry program on the synthesis of dichloroplatinum(II)

complexes that are in a position to form singly and, especially, doubly ring-closed alcoholato species and on investigation of their structures by X-ray crystallography. It was possible to determine the crystal structures of $[\text{Pt}((R)-(-)\text{-HL})_2\text{Cl}_2]$, $[\text{Pt}((S)-(+)\text{-HL})_2\text{Cl}_2]$, $[\text{Pt}((R)-(-)\text{-HL})\{(S)-(+)\text{-HL}\}\text{Cl}_2]$, $[\text{Pt}((S)-(+)\text{-HL})\{(S)-(+)\text{-L}\}\text{Cl}]$, $[\text{Pt}((R)-(-)\text{-L})_2]$ and $[\text{Pt}((S)-(+)\text{-L})_2]$ (HL = 2-aminobutanol- κN , L = 2-aminobutanolato- $\kappa^2\text{N,O}$). The results obtained may represent the first step towards novel prodrugs for platinum-based antitumour chemotherapy.

(© Wiley-VCH Verlag GmbH & Co. KGaA, 69451 Weinheim, Germany, 2003)

Introduction

Alongside the worldwide success of cisplatin [= *cis*-diamminedichloroplatinum(II)] and carboplatin [= *cis*-diammine(1,1-cyclobutanedicarboxylato)platinum(II)] which are routinely used in clinics against certain types of cancer,^[1–5] the so-called third-generation platinum drug oxaliplatin [= *trans*-(1*R*,2*R*)-cyclohexane-1,2-diamine]oxalatoplatinum(II) (Figure 1)] is also today in clinical use.^[6]

In order to overcome the severe side-effects of platinum-based chemotherapy, to improve clinical effectiveness and to broaden the spectrum of activity, there is still a need for other platinum antitumour agents. During recent years, part of the research in this field has focused on platinum(II) and -(IV) complexes with peripheral functional groups. OH- and COOH-substituted ligands were especially of interest because of their potential to act as donors or acceptors for hydrogen bonds, which could play an important role in the binding of platinum compounds to DNA, the major target of platinum-based chemotherapy.^[7] Moreover, these compounds were also used as starting materials for further deri-

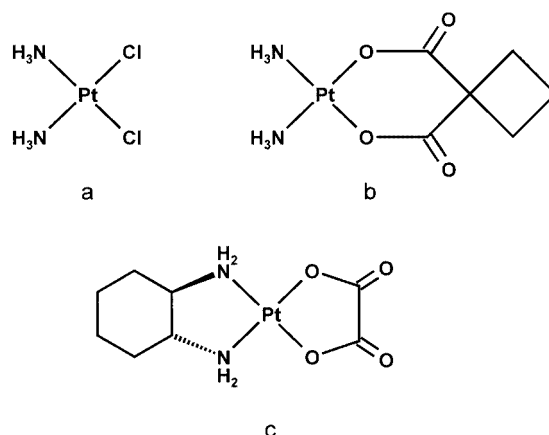


Figure 1. Platinum(II) complexes in clinical use: cisplatin (a), carboplatin (b) and oxaliplatin (c)

vatization,^[8,9] with the aim of attaching suitable carrier molecules for drug targeting.^[10,11]

Hydroxyethyl residues have recently attracted attention because of their ability to coordinate to the platinum centre through the oxygen atom: (i) during oxidation with hydrogen peroxide^[12] or (ii) through an intramolecular ligand exchange reaction in dichloroplatinum(II) complexes.^[13]

In investigation of the binding of potentially cytotoxic platinum coordination compounds to nucleotides, the above intramolecular ligand exchange reaction might at first sight

^[a] Institute of Inorganic Chemistry, Vienna University, Währinger Strasse 42, 1090 Vienna, Austria
Fax: (internat.) + 43-1/4277-52680
E-mail: galanski@ap.univie.ac.at

Supporting information for this article is available on the WWW under <http://www.eurjic.org> or from the author.

be regarded as an undesirable side reaction of a competitive character, complicating the mechanism of action.^[14–16] On the other hand, though, such reactions have also been used specifically for the synthesis of novel tumour-inhibiting platinum(IV) drugs.^[17]

CZE-CE-MS studies have shown^[18] that the binding behaviour of dichlorobis[(2-hydroxyethyl)amine]platinum(II) towards 5'-GMP is dramatically increased by a decrease in the pH from 7.4 to 6.0. This is of great interest in view of the lower pH values encountered in solid tumours and fits with a pH-dependent ring-closing/opening reaction of *N*-(hydroxyethyl)-substituted diaminedichloroplatinum(II) complexes.

The intramolecular ligand exchange reactions described above have been investigated by NMR spectroscopy but there was still a lack of structural information from X-ray crystallography. To fill this gap, and to develop new platinum-based antitumour drugs, we have focused on the synthesis and crystallisation of substituted dichlorobis[(2-hydroxyethyl)amine]platinum(II) complexes and especially their singly and doubly ring-closed species.

Results and Discussion

Synthesis of the bis(2-aminobutanol)dichloroplatinum(II) complexes starts from potassium tetrachloroplatinate(II), K_2PtCl_4 , which is converted in situ to the corresponding tetraiodoplatinate(II) by treatment with KI. After addition either of enantiomerically pure 2-aminobutanol or of the racemic mixture, the (2-aminobutanol)diiodoplatinum(II) compounds are formed. Conversion of the diiodo to the dichloro complexes was performed by treatment of the diiodo compounds with silver nitrate, which afforded the diaminediaquaplatinum(II) species, and subsequent addition of KCl or HCl to provide the bis(2-aminobutanol)dichloroplatinum(II) complexes. Depending on pH, chloride ion concentration and crystallisation, either pure dichloroplatinum(II) complexes, $[Pt(HL)_2Cl_2]$, or a mixture of $[Pt(HL)_2Cl_2]$ and the singly ring-closed species $[Pt(HL)(L)Cl]$ can be isolated (Figure 2). The doubly ring-closed coordination compound could not be detected during this synthetic pathway. The tailor-made synthesis of $[Pt(L)_2]$ was achieved by (i) abstraction of the chloro ligands and (ii) by shifting the pH to values above 7 with a basic ion exchanger.

The purities of the synthesized complexes can best be judged by 1H and ^{13}C NMR spectroscopy. In the case of the enantiomerically pure $[Pt\{(S)-(+)-HL\}_2Cl_2]$ complex, six proton resonances are detected [δ = 0.86 (CH_3), 1.49 (CH_3CH_2), 1.70 (CH_3CH_2), 2.74 (CH), 3.60 (CH_2OH), 4.07 (CH_2OH) ppm]. Because of the asymmetrically substituted methine carbon atom, the two methylene groups show two sets of multiplets, in agreement with their diastereotopic character. Four different ^{13}C signals were found: at δ = 10.0 (CH_3), 24.6 (CH_3CH_2), 59.4 (CH) and 62.5 (CH_2OH) ppm. The corresponding resonances of the doubly ring-closed species were found to be at δ = 0.80 (CH_3), 1.34 (CH_3CH_2),

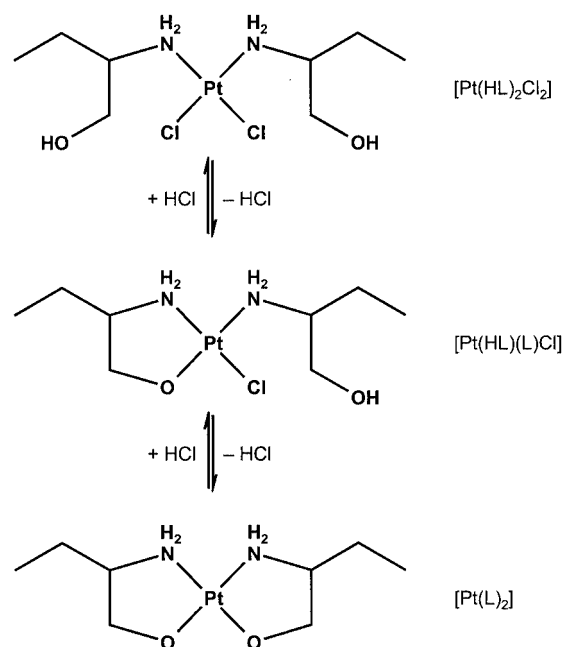


Figure 2. Intramolecular ligand exchange reactions resulting in singly ($[Pt(HL)(L)Cl]$) and doubly ($[Pt(L)_2]$) ring-closed species

1.53 (CH_3CH_2), 2.48 (CH), 2.88 (CH_2O), 3.01 (CH_2O), 10.76 (CH_3), 22.90 (CH_3CH_2), 64.07 (CH) and 73.02 (CH_2O) ppm. Most indicative of the ring-closing reaction are the 1H and ^{13}C chemical shifts of the methylene group next to the oxygen atom. In the chelating (*S*)-(+)-2-aminobutanolato ligands both of the singly and of the doubly ring-closed species, marked shifts of the 1H resonances to higher field and downfield shifts of the ^{13}C signals in relation to the monodentate-coordinated (*S*)-(+)-2-aminobutanol can be seen.

During the synthesis it was possible to isolate crystals suitable for X-ray crystallographic studies. In the presence of hydrochloric acid, compound **1**, $[Pt\{(R)-(-)-HL\}_2Cl_2]$, could be isolated as the dichloroplatinum(II) complex, whereas the structure of **2** {solution of $[Pt\{(S)-(+)-HL\}_2Cl_2]$ in water and KCl} is made up of two different compounds – the dichloroplatinum(II) complex $[Pt\{(S)-(+)-HL\}_2Cl_2]$ and the singly ring-closed species $[Pt\{(S)-(+)-HL\}\{(S)-(+)-L\}Cl]$ – in a 1:1 ratio.

It was also possible to determine the structures of the corresponding doubly ring-closed enantiomerically pure bis(2-aminobutanolato)platinum(II) complexes **3** ($[Pt\{(R)-(-)-L\}_2]$) and **4** ($[Pt\{(S)-(+)-L\}_2]$) in the crystal.

Furthermore, the structure of **S1**, a 1:1 mixture of $[Pt\{(R)-(-)-HL\}\{(S)-(+)-HL\}Cl_2]$ and $[Pt\{(S)-(+)-HL\}_2Cl_2]$ isolated from the synthesis with a racemic mixture of 2-aminobutanol ligands, could also be resolved. Crystal data, data collection parameters and structure refinement details for **S1** are given in Table S4 of the Supporting Information, while the structure is shown in Figure S4.

Figure 3 summarises the results of the single-crystal X-ray structure of one of the two independent molecules of **1**, $[Pt\{(R)-(-)-HL\}_2Cl_2]$. The second independent molecule is shown in Figure S1 in the Supporting Information. The

platinum(II) atom has a square-planar coordination geometry. Two 2-aminobutanol ligands act as neutral monodentate ligands and bind to Pt^{II} through the terminal nitrogen atoms [Pt1–N1 2.057(5), Pt1–N2 2.035(6) Å]. These bond lengths are similar to Pt–N [2.042(4) Å] in Pt^{II}-Cl₂(EA)₂ and shorter than Pt–N [2.070(3) Å] in Pt^{IV}Cl₄(EA)₂·H₂O (EA = ethanolamine).^[19] In addition to two *cis*-disposed organic ligands, two chloride anions Cl1 and Cl2 are bound to Pt^{II} at 2.327(2) and 2.3139(19) Å, respectively. The bond lengths in the coordinated 2-aminobutanol ligands are in a normal range [O1–C1 1.402(10), O2–C5 1.435(9); C1–C2 1.550(13), C5–C6 1.516(10); C2–N1 1.489(9), C6–N2 1.512(9); C2–C3 1.516(9), C6–C7 1.490(9); C3–C4 1.533(13), C7–C8 1.548(11) Å]. Both coordinated NH₂ groups are involved in intramolecular hydrogen bonding (Figure 3) (N1–H1A···O2 with N1–H1A 0.90, H1A···O2 2.121, N1···O2 2.956 Å and N1–H1A···O2 153.77°; and N2–H2A···O1 with N2–H2A 0.90, H2A···O1 2.319, N2···O1 3.049 Å and N2–H2A···O1 138.21°). Both molecules are involved in a three-dimensional hydrogen-bonding network, the packing being dominated by O–H···O, N–H···O and N–H···Cl interactions. Detailed geometrical parameters for the intramolecular contacts in the second independent molecule of **1**, together with intermolecular contacts in **1**, are given in Table S1.

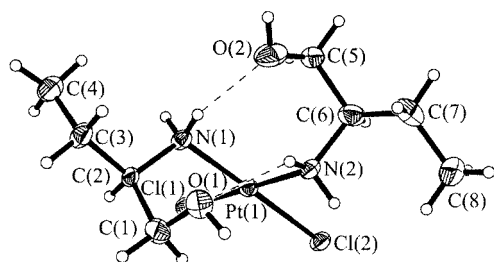


Figure 3. ORTEP diagram of one of the independent molecules of **1** with thermal ellipsoids at 50% probability

The structure of **2** is made up of two different molecules: [Pt{(S)-(+)-HL}₂Cl₂] (**I**) and [Pt{(S)-(+)-HL}{(S)-(+)-L}Cl] (**II**). There are four crystallographically independent molecules in the asymmetric unit: two (A and C) of composition I and two other ones (B and D) of composition II. In addition, molecule C was found to exist in the crystal as two conformers in ca. 0.4:0.6 ratio, differing slightly in the positions of the terminal ethyl groups (Figure S2). The molecular structures of **2-IA** and **2-IIB** are shown in Figures 4 and 5, respectively.

Two neutral 2-aminobutanol ligands act in monodentate fashion and coordinate to Pt^{II} through the terminal amino groups' N1 and N2 atoms in both molecules A and C. They each exhibit a square-planar coordination geometry around Pt, with two nitrogen atoms and two chloride ligands in a *cis* arrangement with average r.m.s. deviations of 0.03 and 0.02 Å, respectively. As in **2-IA** and **2-IC**, the coordination geometry around Pt^{II} in **2-IIB** and **2-IID** can be described as square-planar. The deviation of the coordinated atoms from their mean planes does not exceed 0.04 Å. One neutral 2-aminobutanol ligand acts in monodentate fashion and co-

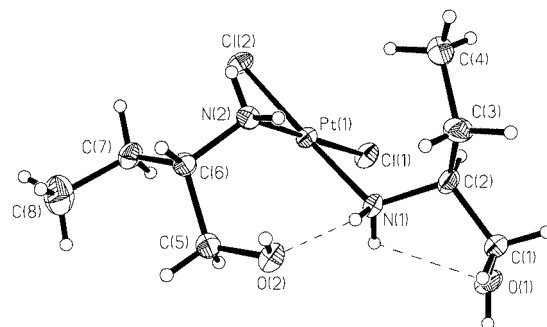


Figure 4. ORTEP diagram of **2-IA** with thermal ellipsoids at 50% probability

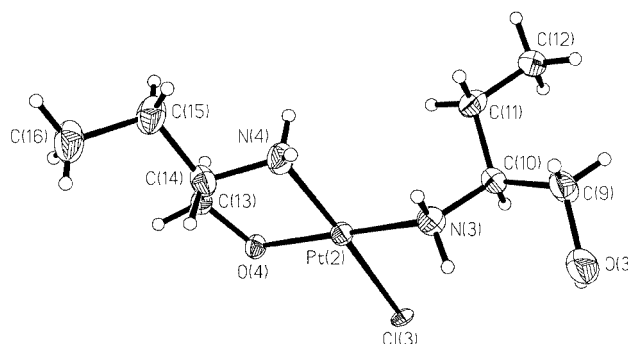


Figure 5. ORTEP diagram of **2-IIB** with thermal ellipsoids at 50% probability

ordinates to Pt^{II} through N3 in **2-IIB** (Figure 5) and through N7 in **2-IID** (Figure S3), whereas another one, deprotonated at the OH group, chelates to the Pt atom through the N4/O4 (**2-IIB**) and N8/O8 (**2-IID**) atoms, giving a *cis* arrangement of amino groups. The fourth coordination place around Pt^{II} in molecules B and D is occupied by chloride anions Cl3 and Cl6, respectively. The chelate ring Pt2O4C13C14N4 in B has an envelope conformation.

The flap^[20] atom protrudes from the plane of the coordinated atoms by 0.63 Å. In contrast, the Pt4O8C29C30N8 chelate ring has a distorted envelope conformation with a weak tendency towards a zigzag arrangement of C29 (+0.09 Å) and C30 (−0.54 Å) (Figure S3). The dihedral angles O4–C13–C14–N4 and O8–C29–C30–N8 compare well, at 48.1(7)° (B) and 50.7° (D). The bite angles, at 82.83(19) and 83.33(19)°, are also similar. The N3–C10 and N7–C26 bonds in the non-chelated ligands in B and D orient almost vertically to the planes of bound platinum atoms with corresponding angles Pt2–N3–C10 and Pt4–N7–C26 at 119.2(4) and 118.6(4)°. All asymmetric carbon atoms in **2** are (*S*)-chiral centres. The corresponding Pt–N, Pt–O and Pt–Cl bond lengths in molecules A, B, C and D as well as the bond lengths in the ligands are quoted in Tables 1 and 2.

Table 1. Bond lengths [Å] in the platinum(II) coordination polyhedron of **2**

Atom1–Atom2	Molecule A	Atom1–Atom2	Molecule C
Pt1–N1	2.057(4)	Pt3–N5	2.065(5)
Pt1–N2	2.061(5)	Pt3–N6	2.060(5)
Pt1–Cl1	2.3080(15)	Pt3–Cl4	2.3102(16)
Pt1–Cl2	2.3264(16)	Pt3–Cl5	2.3283(14)
Atom1–Atom2	Molecule B	Atom1–Atom2	Molecule D
Pt2–O4	2.041(4)	Pt4–O8	2.012(4)
Pt2–N3	2.052(5)	Pt4–N8	2.024(5)
Pt2–N4	2.026(5)	Pt4–N7	2.044(5)
Pt2–Cl3	2.3740(14)	Pt4–Cl6	2.3477(15)

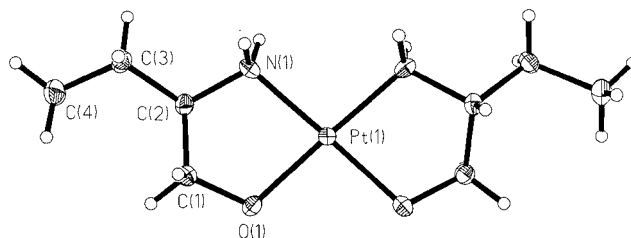
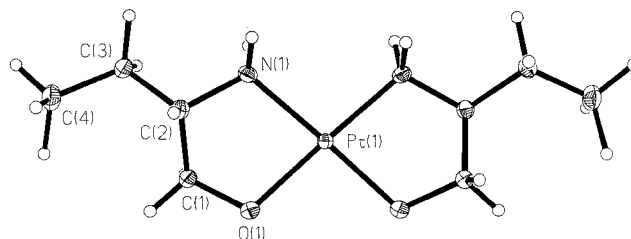
Two intramolecular hydrogen bonds are observed between the amino group of one coordinated 2-aminobutanol ligand as donor and the hydroxy groups of both coordinated HL ligands as acceptors in **A** and **C** (Figures 4 and S1) (N1–H1A···O2 with N1–H1A 0.90, H1A···O2 2.070 Å and N1–H1A···O2 155.34°, and N1–H1B···O1 with N1–H1B 0.90, H1A···O2 2.390 Å and N1–H1A···O2 111.82° in **A**; and N5–H5A···O6 with N5–H5A 0.90, H5A···O6 1.958 Å and N5–H5A···O6 157.72°, and N5–H5B···O5 with N5–H5B 0.90, H5A···O6 2.382 Å and N5–H5A···O6 110.83° in **C**). All four molecules **A**, **B**, **C** and **D** are involved in a three-dimensional hydrogen-bonding network, the packing is dominated by O–H···O, N–H···O and N–H···Cl hydrogen-bonding interactions. Detailed geometrical parameters for the intermolecular contacts in **2** are listed in Table S2.

Both **3** {[Pt{(R)-(–)-L}₂]} and **4** {[Pt{(S)-(+)-L}₂]} crystallize in a non-centrosymmetric orthorhombic space group *P*2₁2₁2. The asymmetric units in **3** and **4** consist of one half of the complex molecule, related to the other by a twofold rotation axis lying in the molecule mean plane across the platinum atom. The results of X-ray crystal structure analyses of **3** and **4** are summarized in Figures 6 and 7.

In both enantiomers [C2 is an (*R*)-chiral centre in **3** and an (*S*)-chiral one in **4**] Pt^{II} has square-planar coordination with two mutually *cis*-arranged 2-aminobutanol ligands deprotonated at the OH group and chelated through NH₂ and O[–]. None of the coordinated atoms protrudes from the corresponding least-squares mean plane by more than 0.002 Å for **3** and 0.004 Å for **4**. Two five-membered chelate rings, with bite angles of 83.31(13) and 83.32(9)° for **3** and **4**, respectively, are formed. A zigzag arrangement of the ligand atoms in the five-membered chelate rings alternately above and below the mean least-squares plane through PtN₂O₂ is observed in both complexes. Unlike in the case of Pt^{IV}(Eta)₂Cl₂,^[21] the two chelate rings PtO1C1C2N1 and the symmetry-related one in the molecules of **3** and **4** are twisted in the opposite sense and their configurations can be described as δλ or λδ. The dihedral angles O1–C1–C2–N1 in **3** and **4**, which serve as measures of the deviation of the corresponding chelate rings from planarity, are –47.1(4) and

Table 2. Bond lengths [Å] in the chelated and non-chelated ligands of **2**

Atom1–Atom2	Molecule B	Atom1–Atom2	Molecule D
O4–C13	1.413(7)	O8–C29	1.413(8)
C13–C14	1.508(9)	C29–C30	1.520(9)
C14–C15	1.561(10)	C30–C31	1.542(9)
C15–C16	1.534(10)	C31–C32	1.487(11)
N4–C14	1.502(8)	N8–C30	1.495(8)
Atom1–Atom2	Molecule A	Atom1–Atom2	Molecule C
O1–C1	1.437(8)	O5–C17	1.435(8)
C1–C2	1.507(8)	C17–C18	1.509(9)
C2–C3	1.519(9)	C18–C19	1.47(3)
C3–C4	1.519(9)	C18–C19X	1.52(2)
N1–C2	1.509(8)	C19–C20	1.548(19)
O2–C5	1.408(7)	C19X–C20X	1.546(18)
C5–C6	1.553(9)	N5–C8	1.483(8)
C6–C7	1.509(9)	O6–C21	1.415(8)
C7–C8	1.539(9)	C21–C22	1.496(9)
N2–C6	1.487(8)	C22–C23	1.516(9)
		C23–C24	1.532(10)
		N6–C22	1.476(8)
Atom1–Atom2	Molecule B	Atom1–Atom2	Molecule D
O3–C9	1.432(9)	O7–C25	1.397(8)
C9–C10	1.524(9)	C25–C26	1.512(9)
C10–C11	1.528(9)	C26–C27	1.491(9)
C11–C12	1.543(9)	C27–C28	1.537(9)
N3–C10	1.488(8)	N7–C26	1.490(8)

Figure 6. ORTEP diagram of **3** with thermal ellipsoids at 50% probabilityFigure 7. ORTEP diagram of **4** with thermal ellipsoids at 50% probability

46.6(3)°, respectively. These values are similar to those in Pt^{IV}(Eta)₂Cl₂. The Pt–O1 and Pt–N1 bond lengths in **3** and **4** compare well, at 2.031(2) and 2.024(2) Å, and 2.029(4) and 2.018(3) Å, respectively. The distributions of electron density over the chelate rings are very similar for

the two enantiomers [O1–C1 at 1.433(5) and 1.434(3), C2–C3 at 1.523(6) and 1.527(4), C3–C4 at 1.524(6) and 1.520(4), N1–C2 at 1.509(5) and 1.500(4) Å for **3** and **4**, respectively].

The NH_2 and the deprotonated OH groups, together with the water molecules, are involved in intermolecular hydrogen bonding, forming a chain of tail-to-head-arranged $\text{Pt}^{\text{II}}\text{L}_2$ molecules (where $\text{HL} = 2\text{-aminobutanol}$), bridged by layers of hydrogen-bonded water molecules and running along the c axis, as shown for **3** in Figure 8.

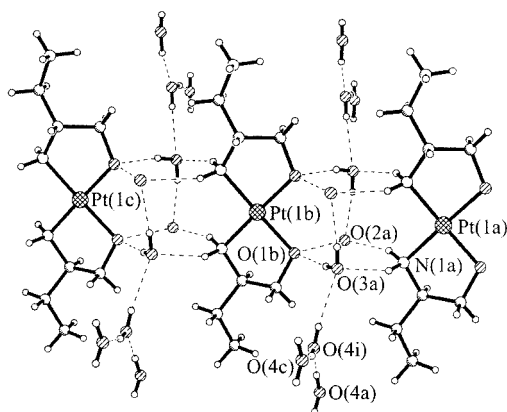


Figure 8. A portion of the crystal structure of **3** projected on the ac plane

Detailed geometrical parameters for the hydrogen bonds in **3** are quoted in Table S3. Another interesting feature is the stacked arrangement of $\text{Pt}^{\text{II}}\text{L}_2$ molecules, with a 4.2 Å intermolecular separation along the b axis (Figure 9). Very weak $\text{C–H}\cdots\text{Pt}$ intermolecular contacts with the C–H vector directed to the platinum atom ($< \text{C–H}\cdots\text{Pt}$ 176.5°) at ca. 3.1 Å are worth mentioning. At ca. 2.6 Å, they are significantly longer than the intramolecular contacts observed in other platinum(II) compounds with square-planar geometries.^[22,23]

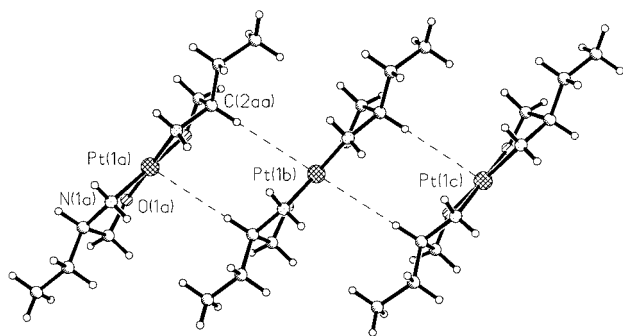


Figure 9. Portion of the crystal structure of **3**, showing stacking arrangement of $\text{Pt}^{\text{II}}\text{L}_2$ along the b axis

Conclusion

Cytotoxic hydroxyethyl-substituted amineplatinum(II) and -(IV) complexes have recently attracted attention because of: (i) the potential of their hydroxy groups to act as donors or acceptors of hydrogen bonds, thus influencing

the mode of action, (ii) their use as starting materials for further derivatisation, and (iii) the ability of their hydroxyethyl groups to coordinate to the platinum centre through the oxygen atom during oxidation with hydrogen peroxide or through intramolecular ligand exchange reactions in dichloroplatinum(II) complexes.

The last point in particular is of great interest, because the intramolecular attack of the hydroxy group dramatically influences the mode of action of platinum(II) compounds, as was shown recently. Moreover, there is the chance to use such reactions specifically for the synthesis of novel anticancer platinum-based drugs for chemotherapy. We have therefore focused our chemistry program on the synthesis of dichloroplatinum(II) complexes that are in a position to form singly or – especially – doubly ring-closed alcoholato species and on investigation of their structures by X-ray crystallography.

The results obtained may represent the first step towards novel prodrugs for platinum-based antitumour chemotherapy.

Experimental Section

General Remarks: All chemicals were obtained from commercial suppliers and used as received. The ^1H and ^{13}C NMR spectra were recorded with a Bruker DPX 400 UltrashieldTM Magnet at 400.13 and 100.62 MHz. The elemental analyses were performed with a Perkin–Elmer 2400 CHN Elemental Analyser by the microlaboratory of the Institute of Physical Chemistry, University of Vienna.

(SP-4–2)-[Bis{(R)-(–)-2-aminobutanol}]diiodoplatinum(II): K_2PtCl_4 (3.621 g, 8.72 mmol) was dissolved in doubly distilled water (35 mL) and treated with KI (7.5 g, 45.18 mmol). The solution was stirred for 20 min at room temperature. A solution of (R)-(–)-2-aminobutanol (1.45 g, 16.27 mmol) in doubly distilled water (10 mL) was added dropwise to the brown suspension of tetraiodoplatinate. After the mixture had been stirred at room temperature for 5 h, $[\text{Pt}\{(R)-(–)\text{-HL}\}_2\text{I}_2]$ was obtained as a precipitate. After filtration, the yellow solid was washed twice with ice-cold water (10 mL). The product was dried over P_4O_{10} . $\text{C}_8\text{H}_{22}\text{I}_2\text{N}_2\text{O}_2\text{Pt}$ (627.18): calcd. C 15.32, H 3.54, N 4.47; found C 15.36, H 3.27 N 4.29. Yield: 2.722 g (50%).

(SP-4–2)-[Bis{(S)-(+)-2-aminobutanol}]diiodoplatinum(II): The synthetic procedure was the same as that used for $[\text{Pt}\{(R)-(–)\text{-HL}\}_2\text{I}_2]$. $\text{C}_8\text{H}_{22}\text{I}_2\text{N}_2\text{O}_2\text{Pt}$ (627.18): calcd. C 15.32, H 3.54, N 4.47; found C 15.29, H 3.36, N 4.92. Yield: 3.4362 g (76%).

[Bis(2-aminobutanol)]diiodoplatinum(II): The synthetic procedure was the same as that used for $[\text{Pt}\{(R)-(–)\text{-HL}\}_2\text{I}_2]$. $\text{C}_8\text{H}_{22}\text{I}_2\text{N}_2\text{O}_2\text{Pt}$ (627.18): calcd. C 15.32, H 3.54, N 4.47; found C 15.02, H 3.30, N 4.25. Yield: 6.848 g (91%).

(SP-4–2)-[Bis{(R)-(–)-2-aminobutanol}]dichloroplatinum(II) (1): $[\text{Pt}\{(R)-(–)\text{-HL}\}_2\text{I}_2]$ (1.5 g, 2.39 mmol) was suspended in doubly distilled water (20 mL). AgNO_3 (0.772 g, 4.54 mmol) was added, and the mixture was stirred for 12 h at room temperature. AgI was removed by filtration. The slightly yellow filtrate was reduced to a volume of 10 mL, and concentrated HCl (1.4 mL, 16.38 mmol) was added. After 5 min, the dichloro complex began to crystallise as yellow needles. ^1H NMR ($\text{H}_2\text{O}/\text{D}_2\text{O}$, 9:1; 1 drop of DCl_{conc}): $\delta = 0.74$ (t, $^3J_{\text{H,H}} = 7.6$ Hz, 6 H, CH_3), 1.28–1.67 (m, 4 H, CH_2CH_2),

2.62 (m, 2 H, CH), 3.51 (m, 2 H, CH₂OH), 3.93 (m, 2 H, CH₂OH) ppm. ¹³C NMR (H₂O/D₂O, 9:1; 1 drop of DCl_{conc}): δ = 10.06 (2 C, CH₃), 24.66 (2 C, CH₃CH₂), 59.34 (2 C, CH), 62.49 (2 C, CH₂OH). C₈H₂₂Cl₂N₂O₂Pt (444.27): calcd. C 21.63, H 4.99, N 6.31; found C 21.56, H 4.87, N 6.17. Yield: 0.55 g (41%).

(SP-4-2)-[Bis{(S)-(+)-2-aminobutanol}]dichloroplatinum(II) and (SP-4-3)-{(S)-(+)-2-aminobutanol}[(S)-(+)-2-aminobutanolato]-κN,O]chloroplatinum(II) (2): [Pt{(S)-(+)-HL}₂Cl₂] (1.8 g, 2.87 mmol) was suspended in doubly distilled water (20 mL). AgNO₃ (0.936 g, 5.51 mmol) was added to the mixture, which was stirred at room temperature for 12 h. AgI was filtered off, and KCl (0.53 g, 7.11 mmol) was added to the slightly yellow filtrate. The colour of the filtrate turned to dark yellow; after 10 min, yellow needles began to crystallise. The mixture was stored at 4 °C for 3 h; 550 mg of a crystalline product could be collected. [Pt{(S)-(+)-HL}₂Cl₂]: ¹H, ¹³C-COSY NMR (H₂O/D₂O, 9:1): δ = 0.86/10.0 (CH₃), 1.49/24.6 (CH₃CH₂), 1.70/24.6 (CH₃CH₂), 2.74/59.4 (CH), 3.60/62.5 (CH₂OH), 4.07/62.5 (CH₂OH). [Pt{(S)-(+)-HL}{(S)-(+)-L}Cl], monodentate ligand: ¹H, ¹³C-COSY NMR (H₂O/D₂O, 9:1): δ = 0.86/10.0 (CH₃), 1.54/22.2 (CH₃CH₂), 1.67/22.2 (CH₃CH₂), 2.78/61.5 (CH), 3.60/62.4 (CH₂OH), 3.95/62.4 (CH₂OH). [Pt{(S)-(+)-HL}{(S)-(+)-L}Cl], bidentate ligand: ¹H, ¹³C-COSY NMR (H₂O/D₂O, 9:1): δ = 0.86/10.0 (CH₃), 1.54/22.2 (CH₃CH₂), 1.67/22.2 (CH₃CH₂), 2.56/60.4 (CH), 3.35/72.6 (CH₂OPT), 3.58/72.6 (CH₂OPT). C₈H₂₂Cl₂N₂O₂Pt·0.1C₈H₂₀ClN₂O₂Pt (485.05): calcd. C 21.79, Cl 15.35, H 5.01, N 6.35; Pt, 43.91; found C 21.50, Cl 15.35, H 4.84, N 6.84; Pt 43.96.

[Bis(2-aminobutanol)]dichloroplatinum(II) (S1): The synthetic procedure was the same as that used for [Pt{(S)-(+)-HL}₂Cl₂]. ¹H NMR (H₂O/D₂O, 9:1; [Pt(HL)₂Cl₂] and [Pt(HL)(L)Cl]): δ = 0.90 (t, ³J_{H,H} = 7.5 Hz, CH₃), 1.42–1.81 (m, CH₃CH₂), 2.48–2.88 (m, CH), 3.32–4.14 (m, CH₂O) ppm. ¹³C NMR (H₂O/D₂O, 9:1; [Pt(HL)₂Cl₂] and [Pt(HL)(L)Cl]): δ = 9.91, 9.95, 10.13, 10.15, 10.30 (CH₃), 22.37, 22.41, 24.49, 24.51, 24.70, 24.77 (CH₃CH₂), 59.51, 60.44, 60.48, 61.47, 61.54 (CH), 65.51, 62.58, 62.75 (CH₂OH), 72.64 (CH₂OPT). C₈H₂₂Cl₂N₂O₂Pt (444.27): calcd. C 21.63, H 4.99, N 6.31; found C 21.72, H 4.79, N 6.25. Yield: 1.390 g (47%).

(SP-4-2)-[Bis{(R)-(-)-2-aminobutanolato}-κ²N,O]platinum(II) (3): [Pt{(R)-(-)-HL}₂Cl₂] (0.3 g) was dissolved in doubly distilled water (10 mL) and treated with rinsed Amberlite IRA-400 (Cl⁻) basic ion exchanger (20 mL). The suspension was stirred at room temperature for 24 h. The ion exchanger was filtered off and the colourless filtrate was concentrated to 1 mL under reduced pressure. The solution was stored over P₄O₁₀ until colourless crystals had formed. ¹H NMR (H₂O/D₂O, 9:1): δ = 0.86 (t, ³J_{H,H} = 7.6 Hz, 4 H, CH₃), 1.42 (m, 2 H, CH₃CH₂), 1.59 (m, 2 H, CH₃CH₂), 2.54 (m, 2 H, CH), 2.94 (m, 2 H, CH₂O), 3.06 (m, 2 H, CH₂O) ppm. ¹³C NMR (H₂O/D₂O, 9:1): δ = 10.78 (2 C, CH₃), 22.89 (2 C, CH₃CH₂), 64.09 (2 C, CH), 73.01 (2 C, CH₂O).

(SP-4-2)-[Bis{(S)-(+)-2-aminobutanolato}-κ²N,O]platinum(II) (4): The synthetic procedure was the same as that used for [Pt{(R)-(-)-L}₂]. ¹H NMR (H₂O/D₂O, 9:1): δ = 0.80 (t, ³J_{H,H} = 7.3 Hz, 6 H, CH₃), 1.34 (m, 2 H, CH₃CH₂), 1.53 (m, 2 H, CH₃CH₂), 2.48 (m, 2 H, CH), 2.88 (m, 2 H, CH₂O), 3.01 (m, 2 H, CH₂O) ppm. ¹³C NMR (H₂O/D₂O, 9:1): δ = 10.76 (s, 2 C, CH₃), 22.90 (s, 2 C, CH₃CH₂), 64.07 (s, 2 C, CH), 73.02 (s, 2 C, CH₂O).

[Bis(2-aminobutanolato)-κ²N,O]platinum(II): The synthetic procedure was the same as that used for [Pt{(R)-(-)-L}₂]. ¹H NMR (H₂O/D₂O, 9:1): δ = 0.79 (t, ³J_{H,H} = 7.3 Hz, 6 H, CH₃), 1.34 (m, 2 H, CH₃CH₂), 1.51 (m, 2 H, CH₃CH₂), 2.46 (m, 2 H, CH), 2.86 (m, 2 H, CH₂O), 3.00 (m, 2 H, CH₂O) ppm. ¹³C NMR (H₂O/D₂O, 9:1): δ = 10.76 (2 C, CH₃), 22.90 (2 C, CH₃CH₂), 64.08 (2 C, CH), 72.90 (2 C, CH₂O). C₈H₂₀N₂O₂Pt·2H₂O (407.38): calcd. C 23.59, H 5.94, N 6.88; found C 23.86, H 5.54, N 6.60. Yield: 0.178 g (71%).

X-ray Crystallographic Study: X-ray diffraction measurements were performed with a Nonius Kappa CCD diffractometer at 120 K. Single crystals were positioned at 35, 40, 35, 35 and 30 mm from the detector and 496, 636, 597, 597 and 414 frames were measured, each for 25, 90, 50, 50 and 65 s over a 2, 1.5, 1.5, 1.5 and 2° scan for **1–4** and **S1**, respectively. The data were processed by use of Denzo-SMN software. Crystal data, data collection parameters, and structure refinement details for **1–4** are given in Table 3. Crystal data, data collection parameters, and structure refinement de-

Table 3. Crystallographic data for **1–4**

Complex	1	2	3	4
Empirical formula	C ₈ H ₂₂ Cl ₂ N ₂ O ₂ Pt	C ₃₂ H ₈₆ Cl ₆ N ₈ O ₈ Pt ₄	C ₄ H ₁₅ NO _{3.5} Pt _{0.5}	C ₄ H ₁₅ NO _{3.5} Pt _{0.5}
Formula mass	444.27	1704.15	230.71	230.71
Space group	monoclinic, <i>P</i> 2 ₁ (no. 4)	monoclinic, <i>P</i> 2 ₁ (no. 4)	orthorhombic, <i>P</i> 2 ₁ 2 ₁ 2 (no. 18)	orthorhombic, <i>P</i> 2 ₁ 2 ₁ 2 (no. 18)
<i>a</i> [Å]	9.9598(3)	10.763(2)	21.527(4)	21.514(4)
<i>b</i> [Å]	9.1516(3)	20.795(4)	5.482(1)	5.481(1)
<i>c</i> [Å]	15.5623(5)	12.072(2)	6.618(1)	6.616(1)
β [°]	107.7389(19)	91.24		
<i>V</i> [Å ³]	1351.03(7)	2701.3(8)	781.0(2)	780.1(2)
<i>Z</i>	4	2	4	4
λ [Å]	0.71073	0.71073	0.71073	0.71073
ρ _{calcd.} [g cm ⁻³]	2.184	2.095	1.962	1.964
Crystal size [mm]	0.11 × 0.10 × 0.10	0.11 × 0.11 × 0.09	0.29 × 0.29 × 0.06	0.23 × 0.22 × 0.04
<i>T</i> [K]	120	120	120	120
μ [cm ⁻¹]	107.67	106.69	90.08	90.18
Flack parameter	0.031(10)	0.012(5)	0.058(15)	0.009(10)
<i>R</i> ^[a]	0.0411	0.0465	0.0307	0.0235
<i>wR</i> ^[b]	0.0755	0.0728	0.0820	0.0561
GOF ^[c]	1.008	0.989	1.108	1.072

[a] *R*1 = Σ(*F*_o - *F*_c)/Σ*F*_o. [b] *wR*2 = {Σ[*w*(*F*_o² - *F*_c²)]/Σ[*w*(*F*_o²)]}^{1/2}. [c] GOF = {Σ[*w*(*F*_o² - *F*_c²)]/(*n* - *p*)}^{1/2}, where *n* is the number of reflections and *p* is the total number of parameters refined.

tails for **S1** are given in Table S4 of the Supporting Information. The structures were solved by direct methods and refined by full-matrix, least-squares techniques. Non-hydrogen atoms were refined with anisotropic displacement parameters. H atoms were calculated and allowed to ride (**1–3** and **S1**) or located on difference Fourier maps (**4**) and isotropically refined, except for those attached to solvate O2 atoms in **3** and **4**, which were not included in the refinements. One of the 2-aminobutanol ligands in **S1** was found to be severely disordered, producing a very short C6–C7 bond and trigonal-planar geometry at C6. Splitting of the atoms C6, C7, C8 and O2 and refinement with a free variable, such that the combined S.O.F. summed to 1.0, resulted in two components with chemically reasonable geometries in a ca. 0.5:0.5 ratio. Both components were modelled by using appropriate SADI restraints to optimize the positions of C6X, C7X, C8X and O2X with respect to C6, C7, C8 and O2. Split atoms were also restrained to have similar anisotropic displacement parameters (ADPs). Redetermination of the structure in the chiral space group $P2_1$ resulted in a distorted geometry and large ADPs. Disorder modelling in one of the independent molecules in **2** required similar SADI restraints and equivalent anisotropic displacement parameters to be applied to the peripheral ethyl group. Two conformers in ca. 0.4:0.6 ratio resulted. Refinement of Flack parameters was useful in assigning the absolute configuration of **2–4**. In all these structures the contribution of the inverted enantiomer is negligible. Computer programs: SHELXS-97^[24] (structure solution), SHELXL-97^[25] (refinement), ORTEP^[26] (molecular diagrams), Pentium II computer, scattering factors.^[27] CCDC-201452 (**1**), -201455 (**2**), -201453 (**3**), -201454 (**4**) and -201456 (**S1**) contain the supplementary crystallographic data for this paper. These data can be obtained free of charge at www.ccdc.cam.ac.uk/conts/retrieving.html [or from the Cambridge Crystallographic Data Centre, 12 Union Road, Cambridge CB2 1EZ, UK; Fax: (internat.) + 44-1223/336-033; E-mail: deposit@ccdc.cam.ac.uk].

Acknowledgments

The support of the FWF (Fonds zur Förderung der wissenschaftlichen Forschung) and COST is gratefully acknowledged. We are thankful to Dr. T. Weyhermüller for the discussion of X-ray data and his suggestions concerning the static disorder in **S1** and to Dr. G. Giester for the collection of X-ray data.

- ^[1] B. Rosenberg, L. VanCamp, T. Krigas, *Nature* **1965**, 205, 698–699.
^[2] B. Rosenberg, L. VanCamp, J. E. Trosko, V. H. Mansour, *Nature* **1969**, 222, 385–386.
^[3] B. Rosenberg, *Interdiscip. Sci. Rev.* **1978**, 3, 134–147.

- ^[4] B. Lippert (Ed.), *Cisplatin: Chemistry and Biochemistry of a Leading Anticancer Drug*, Verlag Helvetica Chimica Acta Zürich (Switzerland) and Wiley-VCH, Weinheim (Germany), **1999**.
^[5] P. J. O'Dwyer, J. P. Stevenson, S. W. Johnson, *Drugs* **2000**, 59 (Suppl. 4), 19–27.
^[6] E. Cvitkovic, M. Bekradda, *Semin. Oncol.* **1999**, 26, 647–662.
^[7] J. Reedijk, *Inorg. Chim. Acta* **1992**, 198–200, 873.
^[8] M. S. Robillard, A. Valentijn, P. M. Rob, N. J. Meeuwenoord, G. A. Van der Marel, J. H. Van Boom, J. Reedijk, *Angew. Chem. Int. Ed.* **2000**, 39, 3096–3099.
^[9] J. N. Jolley, A. I. Yanovsky, L.-R. Kelland, K. B. Nolan, *J. Inorg. Biochem.* **2001**, 83, 91–100.
^[10] L. Cai, K. Lim, S. Ren, R. S. Cadena, W. T. Beck, *J. Med. Chem.* **2001**, 44, 2959–2965.
^[11] M. Galanski, W. Zimmermann, M. Berger, Ch. Baumgartner, G. Giester, B. K. Keppler, *Eur. J. Inorg. Chem.* **2002**, 417–421.
^[12] R. Kuroda, S. Neidle, I. M. Ismail, P. J. Sadler, *J. Chem. Soc., Dalton Trans.* **1983**, 4, 823–825.
^[13] M. Galanski, W. Zimmermann, Ch. Baumgartner, B. K. Keppler, *Eur. J. Inorg. Chem.* **2001**, 5, 1145–1149.
^[14] A. Zenker, M. Galanski, T. L. Bereuter, B. K. Keppler, W. Lindner, *J. Biol. Inorg. Chem.* **2000**, 5, 498–504.
^[15] A. C. G. Hotze, Y. Chen, T. W. Hambley, S. Parsons, N. A. Kratochwil, J. A. Parkinson, V. P. Munk, P. J. Sadler, *Eur. J. Inorg. Chem.* **2002**, 5, 1035–1039.
^[16] M. S. Robillard, M. Galanski, W. Zimmermann, B. K. Keppler, J. Reedijk, *J. Inorg. Biochem.* **2002**, 88, 254–259.
^[17] M. S. Davies, P. N. Wong, A. R. Battle, G. Haddad, M. J. McKeage, T. W. Hambley, *J. Inorg. Biochem.* **2002**, 91, 205–211.
^[18] A. Küng, M. Galanski, Ch. Baumgartner, B. K. Keppler, *Inorg. Chim. Acta* **2002**, 339, 9–13.
^[19] W. Zimmerman, M. Galanski, B. K. Keppler, G. Giester, *Inorg. Chim. Acta* **1999**, 292, 127–130.
^[20] Basic Terminology of stereochemistry (IUPAC Recommendations 1996), *Pure Appl. Chem.* **1996**, 68, 2195–2222.
^[21] R. Kuroda, S. Neidle, I. M. Ismail, P. J. Sadler, *J. Chem. Soc., Dalton Trans.* **1983**, 823–825.
^[22] A. Albinati, C. G. Anklin, F. Ganazzoli, H. Rüegg, P. S. Pregosin, *Inorg. Chem.* **1987**, 26, 503–508.
^[23] A. Albinati, C. Arz, P. S. Pregosin, *Inorg. Chem.* **1987**, 26, 508–513.
^[24] G. M. Sheldrick, SHELXS-97, *Program for Crystal Structure Solution*, University of Göttingen, Germany, **1997**.
^[25] G. M. Sheldrick, SHELXL-97, *Program for Crystal Structure Refinement*, University of Göttingen, Germany, **1997**.
^[26] C. K. Johnson, Rep. ORNL-5138, OAK Ridge National Laboratory, OAK Ridge, TN, **1976**.
^[27] *International Tables for X-ray Crystallography*, Kluwer Academic Press, Dordrecht, The Netherlands, **1992**, vol. C, Tables 4.2.6.8 and 6.1.1.4.

Received January 24, 2003